Thermodynamics and Phase Relations of the Fe-O-S-SiO_2(sat) system at 1200 °C and the Effect of Copper

H. LI and W.J. RANKIN

A laboratory investigation was carried out in which iron was reacted in silica crucibles with an atmosphere of controlled oxygen and sulfur partial pressures. The equilibrium compositions of the melts were determined over the range 10^{-12} to 10^{-9} atm oxygen and $10^{-2.75}$ to 10^{-1} atm sulfur and it was found that the Fe-O-S-SiO_2 system can exist as either a slag or oxysulfide. The oxysulfide contained appreciable quantities of dissolved oxygen and silica, although the levels decreased as the sulfur content was increased. Sulfur also had the effect of reducing the solubility of silica in the slag. When copper was added to the system, the solubility of oxygen and silica in the oxysulfide phase decreased dramatically. The results are examined in terms of the thermodynamics of the relevant reactions, and the predominance area diagram for the copper-free system was established by combining the present results with those of earlier investigations.

I. INTRODUCTION

THE Fe-O-S-SiO_2 system is a fundamental one in nonferrous pyrometallurgy because it is the basis of fayalite slags and iron sulfide-base mattes. The silica-saturated Fe-S-O-SiO_2 system has four components and, according to the phase rule, if the temperature and the partial pressures of oxygen and sulfur are fixed, two phases can coexist: condensed and gas. Because iron can form sulfide (FeS) and oxides (FeO and Fe_2O_3), it is possible for the condensed phase to be present either as a solution of FeO, Fe_2O_3, and SiO_2 containing dissolved FeS (a slag) or as an iron sulfide solution containing dissolved FeO, Fe_2O_3, and SiO_2 (a "matte"). The sulfide phase is frequently referred to as oxysulfide because of its capacity to dissolve oxygen. Silicon is present as silica in both condensed states because under the oxygen and sulfur potentials of matte smelting, silica is the only stable form of silicon. If only one of the oxygen or sulfur potentials is fixed, then slag and oxysulfide phases can coexist.

The silica-free Fe-O-S has been extensively investigated. Hilty and Crafts[1] determined the composition of oxysulfide in the system at equilibrium with iron and established the phase diagram. Bog and Rosenqvist[2] determined the composition of oxysulfide as a function of oxygen and sulfur potential. Stofko *et al.*[3] measured the solubility of oxygen in the system and found that at magnetite saturation the solubility of oxygen was 15.5 pct at 1200 °C.

The sulfur-free FeO-Fe_2O_3-SiO_2 slag system has been studied extensively, but the sulfur-containing Fe-O-S-SiO_2 system has only been studied a little. Ol'Shanskii[4] and Yazawa and Kameda[5] determined the liquidus surface of the portion of the FeS-FeO-SiO_2 system of interest in copper smelting. They found that mixtures of FeS and FeO could form homogeneous melts but that the addition of SiO_2 produced a miscibility gap. In a large part of the system, FeS was soluble in iron silicate liquid to only a limited extent, and excess FeS formed an immiscible sulfide-rich liquid. MacLean[6] studied the liquid phase relations in the FeS-FeO-Fe_3O_4-SiO_2 system and found that iron silicate melts coexisted with iron sulfide melts over a wide range in the experimental system. The solubility of FeS in the iron silicate melt was at a maximum when in equilibrium with iron and it decreased with increasing oxygen potential. An immiscible liquid formed from the excess FeS. MacLean combined his results with those of the earlier studies to construct the phase diagram of the FeO-FeS-SiO_2 system at iron saturation.

Despite the fundamental importance of the Fe-S-O-SiO_2 system in matte smelting, it was investigated extensively only at iron saturation. There have been no experimental investigations to determine the oxygen-sulfur potential boundary between the slag and oxysulfide or the compositions of oxysulfide and slag within their respective fields and at equilibrium. The aim of the present study, therefore, was to determine experimentally the conditions for formation of slag and oxysulfide in the silica saturated Fe-S-O-SiO_2 system at 1200 °C and to determine the effect of oxygen and sulfur potentials on their composition within the slag and oxysulfide fields and when they coexist.

II. EXPERIMENTAL

The experimental approach used was to react a small quantity of iron chips in a silica crucible with a gaseous atmosphere of controlled oxygen and sulfur potential and allow the system to come to equilibrium. The melt was then quenched in air and water and characterized to determine whether the melt was in the slag or oxysulfide state and its elemental composition.

H. LI, formerly with the G.K. Williams Cooperative Research Centre for Extractive Metallurgy, is Associate Lecturer, School of Mathematical and Physical Sciences, Murdoch University, Murdoch, 6150 Australia. W.J. RANKIN, Director, is with the G.K. Williams Cooperative Research Centre for Extractive Metallurgy, University of Melbourne, Parkville, 3052 Australia.

Manuscript submitted January 22, 1993.

A vertical tube furnace heated by silicon carbide elements was used; the tube was impervious mullite with an internal diameter of 40 mm. The silica crucible containing the iron sample was suspended from an alumina tube of 12-mm internal diameter in the constant temperature zone of the furnace. A gas mixture of CO, CO_2, and SO_2 was introduced into the mouth of the crucible through this tube which was also used to raise and lower the reaction crucible. A total flow rate of 400 ml/min was used, and this gave a linear velocity of 60 mm/s through the tube. According to Darken and Gurry,[7] this is the optimum rate for minimizing errors due to thermal segregation, convection currents, and nonequilibrium in the gas mixture. The sample assembly was constructed from three silica crucibles as shown in Figure 1. The outer crucible was supported from the gas inlet tube by means of a thin alumina tube placed horizontally through slots cut into the inlet tube and crucible. The middle crucible was used to protect the outer crucible if the reaction crucible failed. The inner crucible was used to hold the reactants. A type R thermocouple in an alumina sheath was positioned directly below and in contact with the outer crucible and was calibrated at the beginning of the experimental program and at regular intervals against a second thermocouple placed in an empty reaction crucible. The control thermocouple was located on the outside of the mullite work tube. The temperature within the reaction crucible was accurately measured and controlled to within ±3.5 °C at 1200 °C.

The sulfur and oxygen potentials in the furnace were controlled using mixtures of SO_2, CO, and CO_2. High-purity nitrogen was used for flushing the work tube.

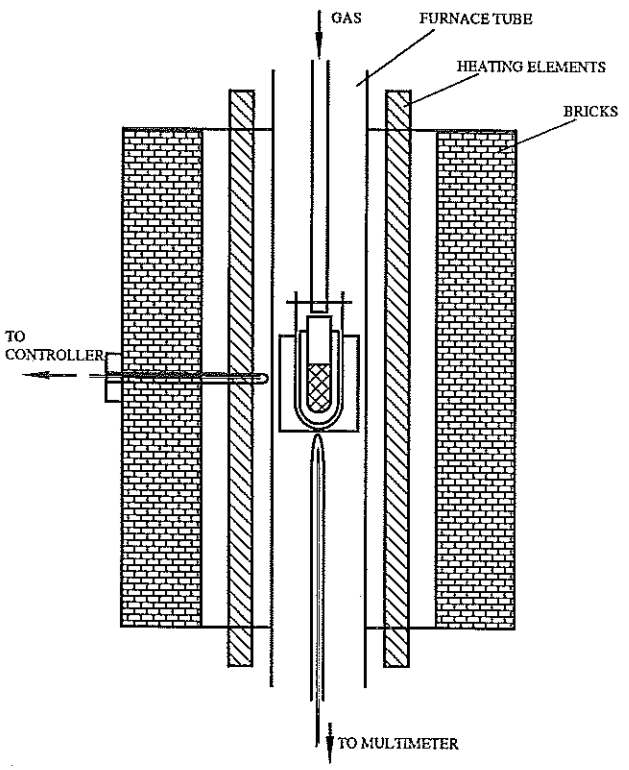

Fig. 1—Furnace configuration used for the experiments.

Gibbs free-energy minimization calculations were performed using the CSIRO Thermochemistry System (with JANAF database) to determine the proportions of these gases required to produce the desired sulfur and oxygen potentials at 1200 °C. The flow rates of the gases were controlled and measured using conventional capillary flow meters and constant-pressure head "bubblers" upstream of the flow meters. All the gases were dried using calcium chloride and magnesium perchlorate, and the carbon dioxide was deoxidized by passing it through a small horizontal tube furnace containing copper wire at 600 °C.

The procedure for an experiment involved placing about 2 g of pure iron chips in the silica reaction crucible and lowering it into the hot zone of the furnace while nitrogen was passed through the tube at 1000 ml/min. When the temperature had stabilized, the nitrogen was replaced by the required mixture of CO, CO_2, and SO_2 at a total flow rate of 400 ml/min. After the reaction period, the atmosphere was changed back to nitrogen, and the reaction crucible was removed rapidly from the furnace and quenched in water. In most of the experiments, there was not a sufficient sample for chemical analysis and an alternative, nondestructive technique was used. The reaction crucible was cut in half lengthwise using a diamond saw, and one piece was mounted in BAKELITE* and polished for microscopic examination. Photomicrographs were taken of all the samples at a magnification of 200 and electron microprobe analyses were performed on selected samples. The photomicrographs were used to determine the nature of each sample (slag or oxysulfide), and the electron microprobe was used to find the composition of the individual species formed during the solidification of the melts. The relative amounts of these species were determined from the photomicrographs and the elemental compositions of the melts were determined by combining this information with the compositions of the individual species. The full details of this technique are given in the Appendix.

*BAKELITE is a trademark of Union Carbide Corporation, Danbury, CT.

III. RESULTS

Two experiments were performed initially to confirm the experimental procedure. The first experiment duplicated that of Darken and Gurry[7] on oxidation of iron. A strip of electrolytic iron was suspended from a Kanthal wire in the hot zone of the furnace and a predetermined mixture of CO and CO_2 was introduced. After 3 hours, the specimen was removed, the position of the boundary between metal and oxidized iron on the strip was measured, and the temperature of the boundary was determined from the measurements of Darken and Gurry. This was repeated three times using different CO-to-CO_2 ratios to establish the temperature profile of the hot zone. The temperature profile obtained this way was compared with the profile measured using a thermocouple, and the difference between the two was within ±2 °C. The second experiment involved duplicating two equilibria performed by Nagamori and Kameda.[8] About 10 g of FeS

Table I. Composition of Samples from the Time Series Experiments

Number	Time Hours	Composition (Wt/Pct)							
		ΣFe	Fe^{2+}	S	O	FeS	FeO	SiO_2	Fe_2O_3
1	1	The iron did not react completely							
2	3	55.9	50.0	1.9	15.8	5.2	59.6	26.9	8.3
3	6	60.1	53.8	12.3	11.9	33.4	41.2	16.3	9.0
4	10	61.6	55.1	13.8	11.6	37.4	39.7	13.7	9.2
5	12	60.6	54.2	13.2	11.6	36.0	39.7	13.7	9.2
6	18	61.3	54.8	13.4	11.7	36.4	40.2	14.3	9.1
7	24	62.0	55.4	14.0	11.6	38.2	39.5	13.1	9.2
8	27	61.5	55.0	13.5	11.7	36.6	40.2	14.0	9.2
9	30	59.9	53.6	13.4	11.3	36.4	38.5	16.1	8.9
10	40	61.4	54.9	13.8	11.5	37.6	39.3	13.9	9.2

was placed in an alumina crucible and equilibrated with a CO-CO_2-SO_2 gas mixture at 1200 °C for 24 hours. The sample was quenched and then analyzed for its total iron and sulfur contents; the oxygen content was determined by difference. The results for the experiments performed agreed within ±7 pct with those of Nagamori and Kameda. These experiments were taken as confirmation that the experimental system was performing satisfactorily.

A. *Approach to Equilibrium*

The time required for equilibrium to be attained was determined in a second series of experiments performed at a partial pressure of oxygen of $10^{-10.5}$ atm and a partial pressure of sulfur of $10^{-2.0}$ atm. As subsequent tests revealed, these conditions placed the system in the oxysulfide field. The results for these tests are given in Table I and are shown graphically in Figure 2 from which it is apparent that equilibrium was attained in about 6 hours. Accordingly, subsequent runs were performed for 10 hours. The sequence of reactions can be clearly seen from the trends in Figure 2. The metallic iron first reacted with oxygen in the gas to form FeO, then the FeO reacted with silica from the crucible to form fayalite slag, and, finally, silica was rejected from the melt as the fayalite changed to oxysulfide by reaction with sulfur in the gas. This sequence of reactions was also apparent in the photomicrographs of samples from this series.

B. *Effect of Oxygen and Sulfur Partial Pressure*

A series of 48 experiments was performed in which the oxygen and sulfur partial pressures were systematically varied over the range $p_{O_2} = 10^{-9.0}$ to $10^{-12.0}$ atm and $p_{S_2} = 10^{-1.0}$ to $10^{-2.75}$ atm. The equilibrium compositions of the melts and the corresponding oxygen and sulfur partial pressures are given in Table II.

The photomicrographs revealed that there were two types of microstructure: one with a light matrix phase and the other with a dark matrix phase. Typical examples are shown in Figures 3 and 4. The electron microprobe analyses indicated that the light phase was nearly pure FeS and that the dark phase was nearly pure fayalite ($2FeO \cdot SiO_2$). The samples classified into the two types of microstructure are shown in Figure 5, and it is clear that there is a sharp division according to the oxygen and sulfur partial pressures. A few samples were difficult to classify, and these are indicated with a question mark in the figure.

The variation of the sulfur content of the melts at constant partial pressure of sulfur (vertical sections through Figure 5) and at constant oxygen partial pressure (horizontal sections through Figure 5) are shown in Figures 6 and 7, respectively. There is clearly a discontinuity in the sulfur concentration, and this corresponds to the boundary in Figure 5 between the two microstructure types. This indicates that the melt existed in two distinct states during the experiment and that the microstructures do not only reflect conditions during solidification. The open triangles in Figure 5 correspond to the slag state at 1200 °C, while the closed squares correspond to the oxysulfide state.

The variation of the slag composition (expressed in terms of mass percent FeO, Fe_2O_3, FeS, and SiO_2) with change in sulfur partial pressure is shown in Figure 8 for oxygen partial pressures of $10^{-9.0}$, $10^{-9.5}$, and 10^{-10} atm. The trends are the same at the different oxygen partial pressures, but the lines are displaced slightly. At the lowest sulfur partial pressure (10^{-3} atm), the slags contain about 1.5 pct FeS (0.5 pct S), 7 to 9 pct Fe_2O_3, 31 to 33 pct SiO_2, and the balance FeO. The FeS content increases with increasing sulfur partial pressure, while the SiO_2 and FeO contents decrease. The Fe_2O_3 content of the slag is independent of the sulfur partial pressure and decreases slightly as the oxygen partial pressure decreases from 10^{-9} to 10^{-10} atm.

If the oxysulfide is considered as a solution of Fe, S, O, and SiO_2, the oxygen concentration varies from 7.5 to 12.0 pct as shown in Figure 9. There is considerable scatter in the data because it covers oxygen partial pressures from 10^{-9} to 10^{-11} atm, but there appears to be a slight decrease in oxygen content of the oxysulfide as the sulfur partial pressure increased. The oxysulfide may also be considered as a solution of FeO, Fe_2O_3, FeS, and SiO_2, and the variation in concentration of these species with sulfur partial pressure is shown in Figure 10 at a partial pressure of oxygen of 10^{-10} atm. Similar trends are exhibited at oxygen partial pressures of $10^{-9.5}$ and $10^{-9.0}$ atm. The relations have been extrapolated from the highest experimental partial pressure of sulfur of 10^{-1} to 1 atm in order to show the expected composition at 1 atm. Over the range investigated experimentally, the

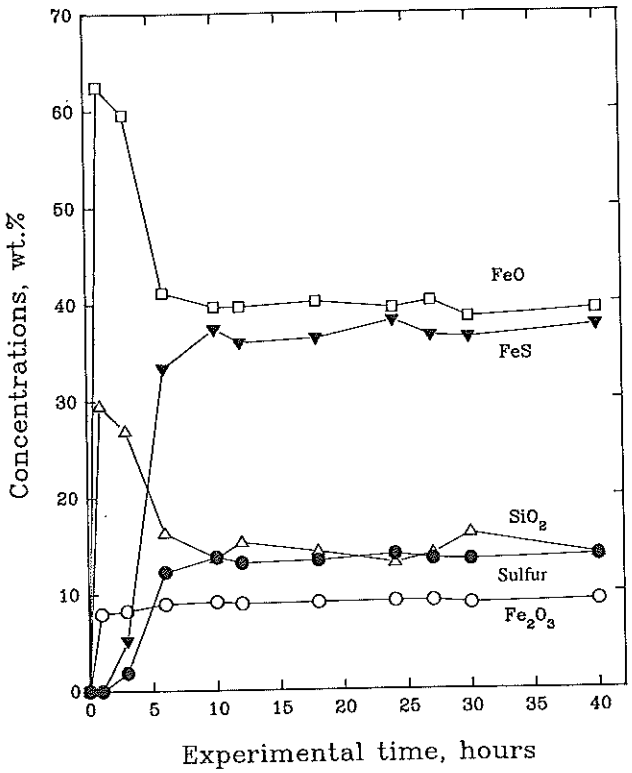

Fig. 2—Approach to equilibrium of the melt with gas (p_{O_2} = $10^{-10.5}$ atm, p_{S_2} = $10^{-2.0}$ atm).

silica solubility in oxysulfide decreases from about 13 pct at a sulfur partial pressure of $10^{-1.75}$ atm to about 7 pct at 10^{-1} atm. The extrapolation indicates that the solubility of silica in FeS should be very small at a sulfur partial pressure of 1 atm and this is consistent with observations (pure FeS is frequently prepared in the laboratory by heating a mixture of iron powder and sulfur in a sealed silica capsule). The FeS content of the oxysulfide increases rapidly with increasing sulfur partial pressure, and there is a corresponding decrease in FeO content as sulfur replaces oxygen in the system. The Fe_2O_3 content is independent of the sulfur partial pressure and has a value of approximately 10 pct.

C. *Effect of Addition of Copper*

Copper matte is the most common sulfide melt in practice, and the Fe-O-S-SiO_2 system is a subsystem of copper matte. Because of the addition of copper, the number of degrees of freedom in the system was increased by one and, when both oxygen and sulfur potentials are fixed, in this case both slag and matte can coexist. Three experiments, at different oxygen and sulfur partial pressures, were performed in which copper in the form of CuS was added with the iron chips in the silica crucible. The experiments were performed in the same manner as for the copper-free experiments. In these experiments, however, there was little attack on the crucible, and sufficient slag and matte were recovered at the end of the reaction to enable chemical analyses to be carried out. The conditions of the experiments and the analyses of the slag and matte are given in Table III. The copper content of the matte is 50 to 58 pct. The oxygen and silica contents are low compared with the copper-free system, 0.4 to 1.4 pct and 1.0 to 2.0 pct, respectively, and it is clear that copper in the sulfide phase has a great effect on oxygen and silica solubility.

IV. DISCUSSION

The sulfur-free FeO-Fe_2O_3-SiO_2 slag system has been extensively investigated, and the phase data for the system have been compiled by Muan and Osborn[9] to produce the commonly accepted phase diagram. According to this diagram, silica-saturated slags containing approximately 10 pct Fe_2O_3 contain about 35 pct silica at 1200 °C. The results of Schuhmann[10] show that sulfur-free silica-saturated slags at oxygen partial pressures of 10^{-9} to 10^{-10} atm contain 35 to 37 pct silica at 1200 °C. Slags from the present study with the lowest sulfur content (about 0.5 pct) contained 32 to 34 pct silica, and the silica content decreased as the sulfur content increased. The silica content of the slags from the experiments which contained 3.0 to 3.7 pct copper was 30.0 to 32.5 pct for slags containing 3.6 to 2.4 pct S. It can be concluded that sulfur decreases the solubility of silica in silica-saturated FeO-Fe_2O_3-SiO_2 slags.

The results show that silica solubility in the oxysulfide phase has a strong direct correlation with the oxygen (or FeO) content. The oxygen content is inversely proportional to the sulfur content and as the sulfur partial pressure is increased, both the oxygen and silica contents decrease. The relatively high silica content of the oxysulfide can be explained by the strong propensity of FeO and silica to form fayalite. As the sulfur content of oxysulfide increases, the amount of iron as FeO decreases due to formation of FeS and the oxygen content decreases. As the FeO content decreases so, therefore, does the silica content. When copper was added to the system, both the oxygen and silica contents of the oxysulfide decreased. This would be expected if copper decreases the solubility of oxygen. The replacement of some iron by copper should decrease the solubility of oxygen because copper has a stronger propensity than iron to form sulfide rather than oxide.[11]

$$\mathrm{FeO\ (s)} + \frac{1}{2}\mathrm{S_2\ (g)} = \mathrm{FeS\ (s)} + \frac{1}{2}\mathrm{O_2\ (g)};$$

$$\Delta G^\circ_{1473} = 96{,}300\ \mathrm{J} \qquad [1]$$

$$\mathrm{Cu_2O\ (s)} + \frac{1}{2}\mathrm{S_2\ (g)} = \mathrm{Cu_2S\ (s)} + \frac{1}{2}\mathrm{O_2\ (g)};$$

$$\Delta G^\circ_{1473} = -25{,}500\ \mathrm{J} \qquad [2]$$

The iron contents of the copper mattes produced in the experiments are about one-third those of the copper-free oxysulfide, and if copper acted simply as a dilutent then the oxygen contents of the mattes should also be about one-third those of the oxysulfide, *i.e.*, about 2.5 to 4.5 pct. In fact, the oxygen content of the mattes is

Table II. Composition of the Samples from the Experiments Performed for 10 Hours

Number	p_{O_2}	p_{S_2}	Composition (Wt Pct)							
			ΣFe	Fe^{2+}	S	O	FeS	FeO	SiO_2	Fe_2O_3
11	$10^{-9.0}$	$10^{-1.0}$	56.8	49.6	3.7	15.3	10.2	54.9	24.8	10.1
12		$10^{-1.5}$	54.1	47.3	3.5	14.6	9.6	52.4	28.4	9.6
13		$10^{-2.0}$	54.9	48.0	2.2	15.4	6.1	56.1	28.0	9.8
14		$10^{-2.25}$	54.6	47.7	1.9	15.5	5.2	56.5	28.6	9.7
15		$10^{-2.5}$	54.5	47.6	1.2	15.8	3.2	58.1	29.0	9.7
16		$10^{-2.75}$	53.5	46.8	1.0	15.6	2.6	57.4	30.4	9.5
17	$10^{-9.25}$	$10^{-1.0}$	63.6	55.8	17.0	10.7	46.1	33.4	9.6	10.9
18	$10^{-9.5}$	$10^{-1.0}$	63.5	56.0	19.1	9.6	51.8	28.9	8.6	10.6
19		$10^{-1.25}$	62.4	55.0	16.2	10.7	43.9	34.1	11.5	10.4
20		$10^{-1.5}$	57.6	50.8	4.8	15.0	12.9	54.2	23.3	9.6
21		$10^{-2.0}$	54.6	48.1	3.0	14.9	8.1	54.7	28.1	9.1
22		$10^{-2.25}$	53.6	47.2	2.4	14.9	6.5	54.9	29.7	8.9
23		$10^{-2.5}$	53.8	47.5	1.5	15.5	4.0	57.3	29.7	9.0
24		$10^{-2.75}$	54.7	48.3	1.7	15.6	4.5	57.8	28.5	9.1
25	$10^{-9.75}$	$10^{-1.0}$	62.9	55.7	21.7	8.1	58.9	22.8	8.1	10.2
26		$10^{-1.25}$	62.1	55.0	17.1	10.2	46.4	32.1	11.5	10.1
27		$10^{-1.5}$	62.2	55.1	14.4	11.5	39.1	38.2	12.6	10.1
28		$10^{-1.75}$	56.6	50.1	4.4	14.8	12.1	54.0	24.8	9.2
29	$10^{-10.0}$	$10^{-1.0}$	63.5	56.4	21.5	8.4	58.4	24.1	7.5	10.0
30		$10^{-1.0}$	63.4	56.3	21.3	8.5	57.8	24.4	7.9	9.8
31		$10^{-1.25}$	62.6	55.6	18.3	9.7	49.8	30.1	10.2	9.8
32		$10^{-1.5}$	61.3	54.5	14.8	11.0	40.2	36.6	13.6	9.6
33		$10^{-1.75}$	61.9	55.0	14.2	11.5	38.7	38.5	13.1	9.8
34		$10^{-2.0}$	55.8	49.5	3.4	15.0	9.2	55.7	26.4	8.8
35		$10^{-2.25}$	54.0	48.0	2.6	14.9	7.1	55.4	29.0	8.5
36		$10^{-2.5}$	55.0	48.9	1.4	15.8	3.8	59.2	28.3	8.7
37		$10^{-2.75}$	52.1	46.3	1.4	14.9	3.7	56.0	32.0	8.2
38	$10^{-10.25}$	$10^{-1.5}$	63.2	56.3	16.6	10.7	45.0	35.0	10.3	9.7
39		$10^{-1.75}$	61.1	54.5	14.9	10.9	40.5	36.4	13.7	9.4
40		$10^{-2.0}$	58.3	52.0	8.4	13.3	22.7	47.7	20.7	8.9
41	$10^{-10.5}$	$10^{-1.5}$	60.4	54.0	15.5	10.4	42.2	34.4	14.4	9.0
42		$10^{-1.75}$	60.7	54.3	14.7	10.9	40.0	36.6	14.4	9.0
43		$10^{-2.0}$	59.7	53.4	13.6	11.1	37.0	37.9	16.2	8.9
44		$10^{-2.25}$	56.8	50.8	3.4	15.3	9.4	57.1	25.0	8.5
45		$10^{-2.5}$	54.4	48.7	1.7	15.4	4.7	58.3	28.9	8.1
46		$10^{-2.75}$	52.8	47.2	1.4	15.1	3.8	57.1	31.2	7.9
47	$10^{-10.75}$	$10^{-2.0}$	61.8	55.5	14.4	11.3	39.3	38.6	13.1	9.0
48		$10^{-2.25}$	61.2	54.9	13.0	11.8	35.4	41.1	14.6	8.9
49		$10^{-2.5}$	56.0	50.2	1.6	15.9	4.4	60.5	26.9	8.1
50	$10^{-11.0}$	$10^{-2.0}$	61.1	55.0	15.8	10.4	43.1	35.0	13.3	8.6
51		$10^{-2.25}$	60.6	54.6	13.8	11.2	37.6	38.9	14.9	8.6
52		$10^{-2.5}$	61.8	55.6	13.0	12.0	35.5	41.9	13.8	8.8
53		$10^{-2.75}$	57.2	51.5	4.1	15.0	11.2	56.5	24.2	8.1
54	$10^{-11.25}$	$10^{-2.25}$	59.8	54.0	13.9	10.9	37.8	38.0	15.9	8.3
55		$10^{-2.5}$	60.9	54.9	14.1	11.1	38.4	38.7	14.5	8.4
56	$10^{-11.5}$	$10^{-2.5}$	62.9	57.0	17.2	10.2	46.8	34.4	10.3	8.5
57	$10^{-12.0}$	$10^{-2.0}$	63.8	58.0	23.1	7.5	62.8	22.8	6.2	8.2
58	$10^{-10.0}$	No sulfur	55.6	49.4	0.03	16.6	0.07	52.9	28.2	8.8

closer to 1 pct; this suggests that Cu_2S and FeS interact in the matte in a way to lower the activity of FeS below that for an ideal solution of the two.

The decrease in oxygen solubility in matte with increasing copper content has been observed by previous workers.[12–15] The present results for oxygen content of copper-containing mattes are very similar to those of Bor and Tarassof[12] and Gevici and Rosenqvist[13] but are about half the values found by Tavera and Davenport.[14] The copper-free oxysulfide values from this study are also consistent with values for low-copper and copper-free mattes obtained by Spira and Themelis[15] who found oxygen contents in mattes of 5 to 10 pct for copper contents from 25 to 0 pct, respectively. The "cleaner" separation of mattes from slags at high copper contents of matte is well known,[16] and the explanation for this, therefore, is likely to be the low silica solubility in mattes at high copper contents.

The discontinuities in the curves in Figures 6 and 7 provide a means of accurately determining the oxygen and sulfur partial pressures at which slag and oxysulfide coexist. These can then be used to construct the boundary between slag and oxysulfide on the predominance area diagram for the Fe-O-S-SiO_2(sat). This is shown as

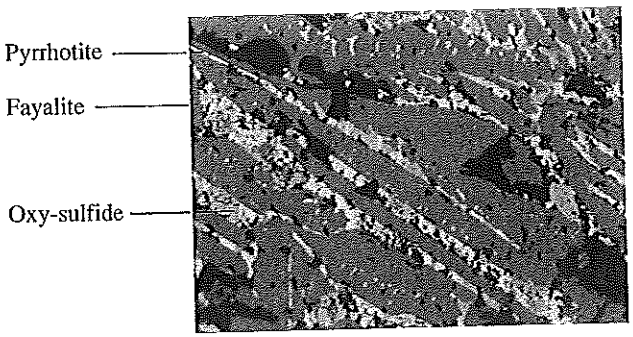

Fig. 3—Typical photomicrograph of quenched melt with the slag structure (magnification 200 times).

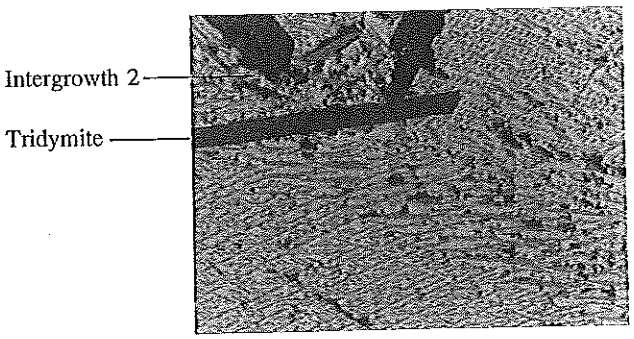

Fig. 4—Typical photomicrograph of quenched melt with the oxy-sulfide structure (magnification 200 times).

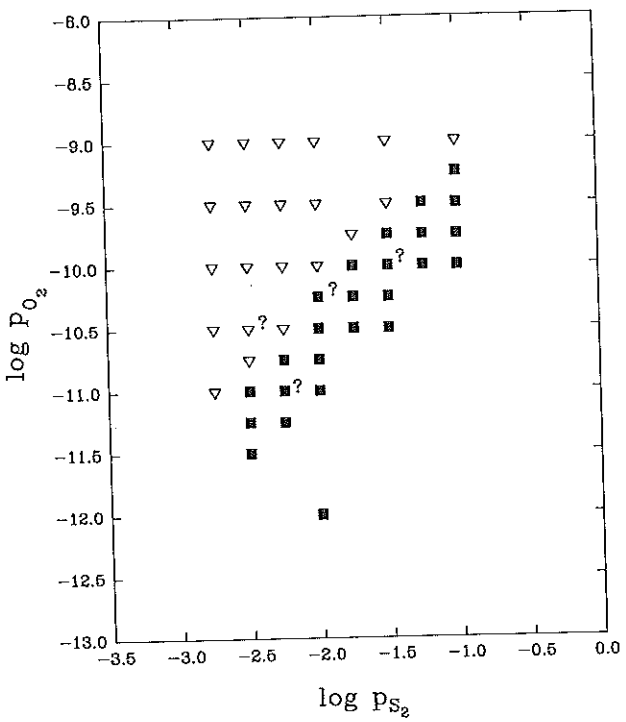

Fig. 5—Classification of quenched melts according to the nature of the matrix phase. Open triangles indicate fayalite matrix, and closed squares indicate iron sulfide matrix.

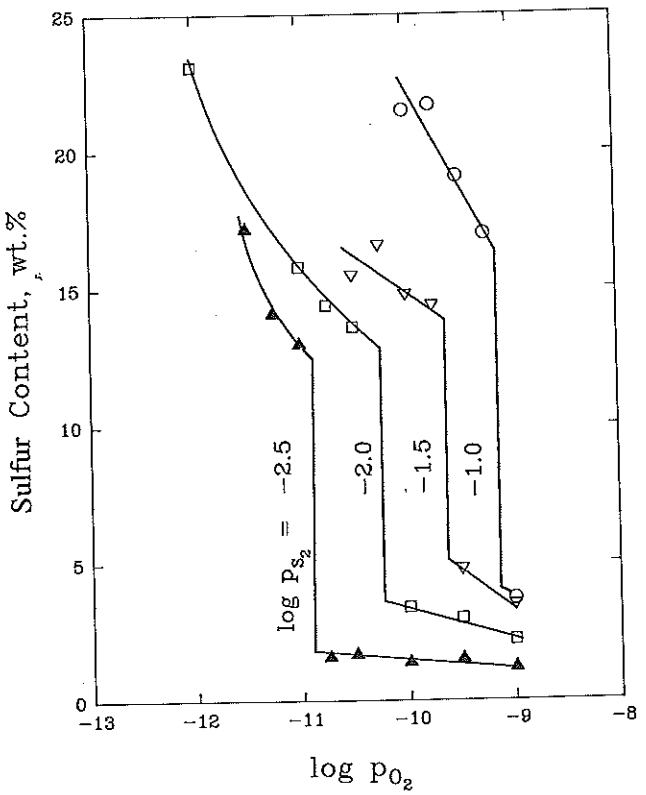

Fig. 6—The effect of oxygen partial pressure on the sulfur content of melts at constant sulfur partial pressure.

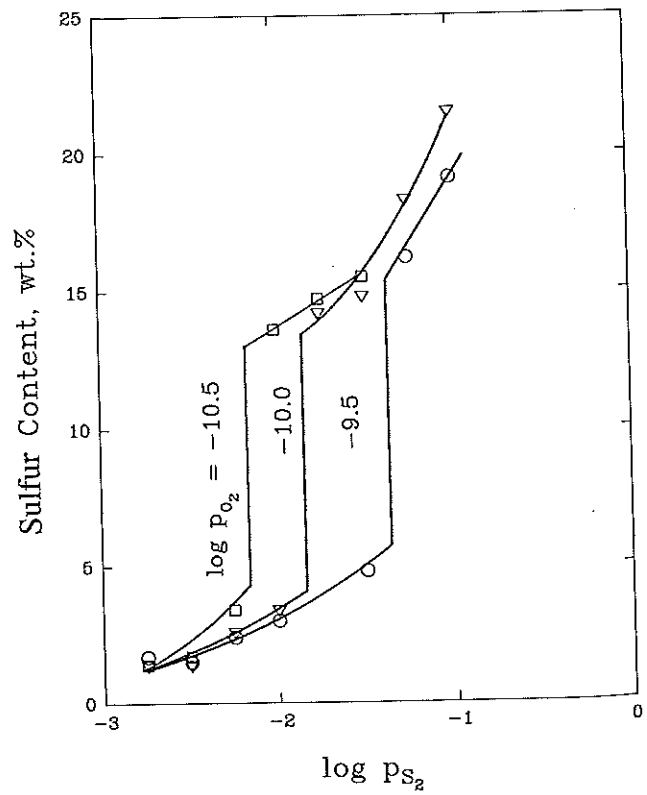

Fig. 7—The effect of sulfur partial pressure on the sulfur content of melts at constant oxygen partial pressure.

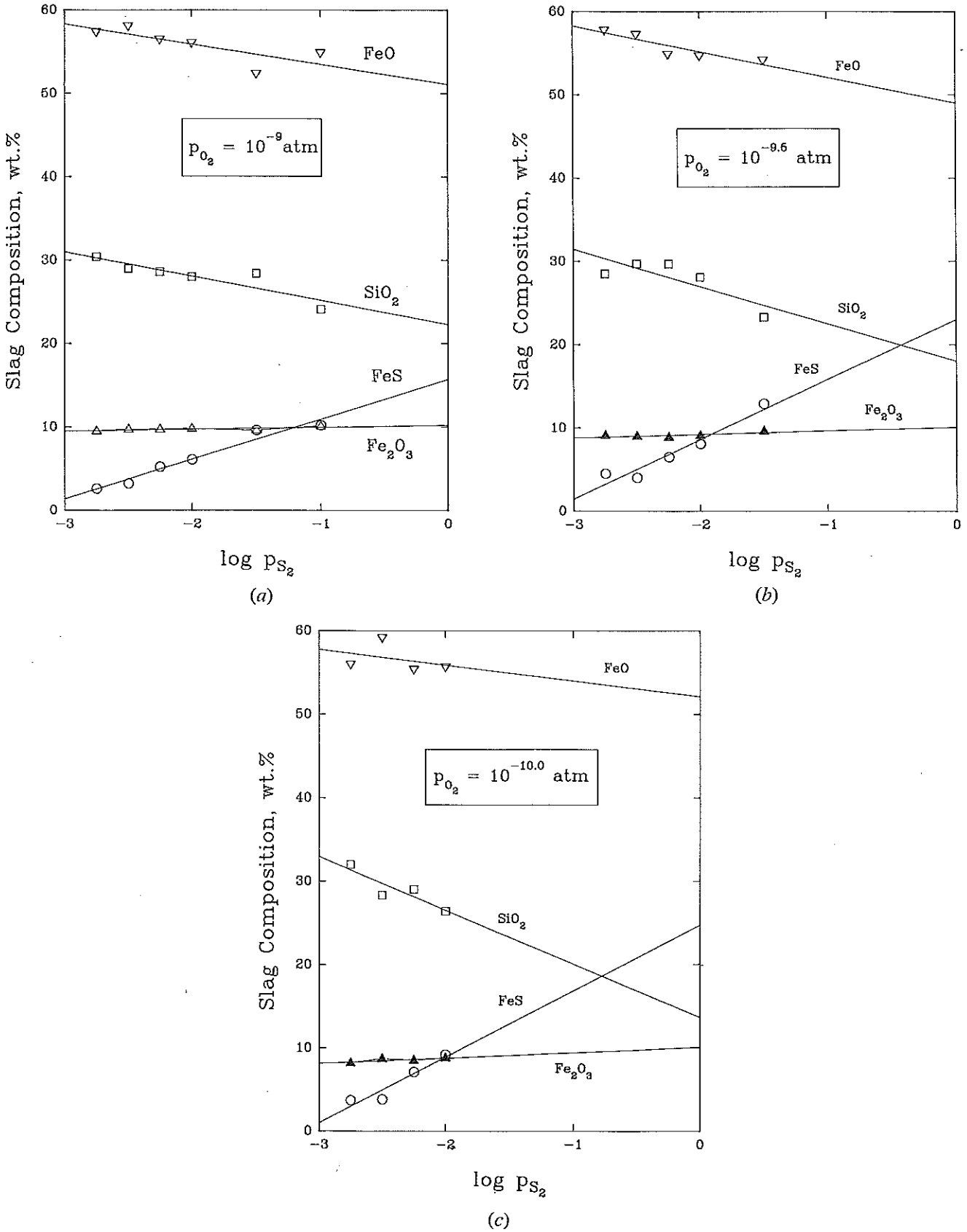

Fig. 8—Effect of partial pressure of sulfur on the slag composition at $10^{-9.0}$, $10^{-9.5}$, and $10^{-10.0}$ atm.

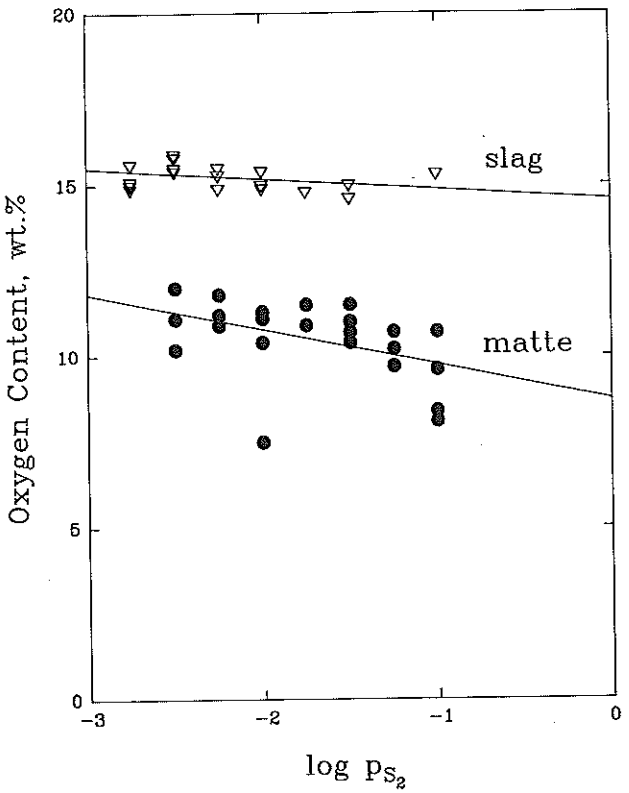

Fig. 9—Effect of sulfur partial pressure on the oxygen content of oxysulfide and slag at oxygen partial pressures of 10^{-9} to 10^{-11} atm.

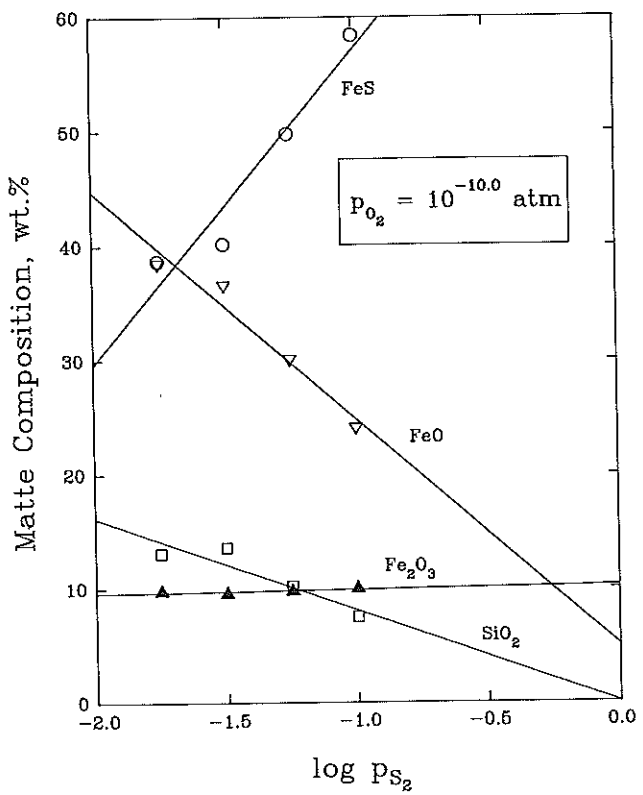

Fig. 10—Effect of sulfur partial pressure on the composition of oxysulfide at oxygen partial pressure of 10^{-10} atm.

the section OP in Figure 11. Other lines have also been drawn in the figure to complete the predominance area diagram over the range of oxygen and sulfur partial pressures of practical interest. The line HY is given by

$$\log p_{S_2} = -5.08 + 2 \log a_{FeS} \qquad [3]$$

which represents the equilibrium of the following reaction:[17]

$$\text{Fe (s)} + \frac{1}{2}\text{S}_2\text{ (g)} = \text{FeS (l)};$$

$$\Delta G^\circ = -116{,}270 + 30.33\,T\text{ J} \qquad [4]$$

The activity of FeS in FeS melts in equilibrium with solid iron is 0.66 to 0.69.[18,19] Although these values were obtained for the oxygen-free system, it is reasonable to assume that the oxygen content of FeS is negligible below oxygen partial pressures of 10^{-13} atm.

The line SY represents the equilibrium between solid iron and FeO[20] at 1200 °C.

$$\text{Fe (s)} + \frac{1}{2}\text{O}_2\text{ (g)} = \text{FeO (l)};$$

$$\Delta G^\circ = -231{,}980 + 45.54\,\text{T J} \qquad [5]$$

Therefore,

$$\log p_{O_2} = -11.71 + 2 \log a_{FeO} \qquad [6]$$

Schumann and Ensio[21] determined the activity of FeO to be 0.41 in fayalite slags saturated with both silica and iron. This value was used to locate point S on the assumption that FeO activity is not affected by sulfur at partial pressures of sulfur below 10^{-7} atm. Yazawa[19] determined the activities of FeS and FeO in iron- and silica-saturated slag in equilibrium with oxysulfide at 1200 °C to be 0.66 and 0.30, respectively. These values were used to locate point Y. The comparable values of 0.69 and 0.36 obtained by Nagamori *et al.*[18] do not alter the position significantly. The curve SYOP was obtained by joining points S, Y, and O with a smooth curve to join with the experimentally determined curve OP. The curve SYOP represents the equilibrium between slag and oxysulfide as a function of oxygen and sulfur partial pressures obtained by combining Eqs. [4] and [5]:

$$\text{FeO (l)} + \frac{1}{2}\text{S}_2\text{ (g)} = \text{FeS (l)} + \frac{1}{2}\text{O}_2\text{ (g)};$$

$$\Delta G^\circ = 115{,}710 - 15.21\,\text{T J}$$

The curve is given by the following relation:

$$\log \frac{a_{FeS}}{a_{FeO}} = -3.31 + 0.5 \log \frac{p_{S_2}}{p_{O_2}}$$

The variation of the activity ratio of FeS-to-FeO for the section YOP is shown in Figure 12. Clearly, the sulfur content of slag and oxysulfide has a marked effect on the activities of FeO and FeS. It would be expected that the activity of FeS would increase as sulfur content increased and that the activity of FeO would decrease. It should be noted that the relation in Figure 12 applies

Table III. Conditions for Copper-Containing Experiments and Results of Analysis of the Slags and Mattes

p_{O_2}	p_{S_2}		Pct Cu	Pct S	Pct ΣFe	Pct O	Pct SiO_2
$10^{-9.125}$	$10^{-1.0}$	slag	3.55	3.6	46.9	16.0	30.0
		matte	50.0	24.7	23.9	0.4	1
$10^{-10.25}$	$10^{-2.0}$	slag	3.0	3.1	45.8	15.5	32.6
		matte	51.7	23.6	22.2	0.6	1.95
$10^{-10.875}$	$10^{-2.5}$	slag	3.7	2.4	46.0	15.4	32.5
		matte	58.0	22.3	17.1	1.4	1.25

Note: Oxygen contents were obtained by difference.

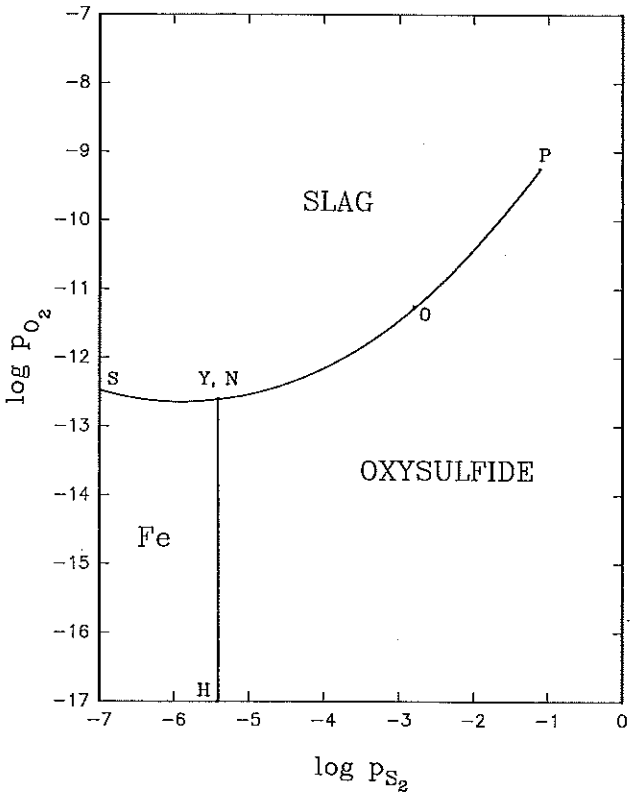

Fig. 11—Predominance area diagram of the Fe-S-O-SiO_2 (sat) system at 1200 °C.

to the FeO and FeS contents of both the slag and oxysulfide along YOP since, at equilibrium, the activity of a species is the same in both phases.

V. CONCLUSIONS

The Fe-O-S-SiO_2(sat) system can exist in two states depending on the oxygen and sulfur potential: slag and oxysulfide. These phases can coexist only at unique combinations of oxygen and sulfur potential. In Fe-Fe_2O_3-SiO_2(sat) slags, increasing the sulfur content from 0.5 to 5 pct had the effect of decreasing the silica content from about 32 pct to 20 to 25 pct at partial pressures of oxygen of 10^{-9} to 10^{-10} atm. The solubility of oxygen in oxysulfide was in the range 7.5 to 12 pct and that of silica in a range 7 to 13 pct. Both oxygen and silica solubility decreased as the sulfur content of the oxysulfide increased.

The addition of copper to the system reduced the solubility of oxygen and silica in the oxysulfide (matte) to very low levels. Oxygen and silica in both slag and oxysulfide appear to be associated through their tendency to form fayalite in the presence of iron. When sulfur replaces some of the oxygen, therefore, the solubility of silica decreases. When copper replaces some of the iron in the oxysulfide, the oxygen, and hence silica solubility, is reduced because copper has a greater tendency to form sulfide than does iron.

The predominance area diagram has been determined for the copper-free, silica-saturated system by combining the results from this work with those of other investigations. Values of the ratio of the activities of FeS and FeO along the boundary between slag and oxysulfide have been estimated, and they show a considerable variation.

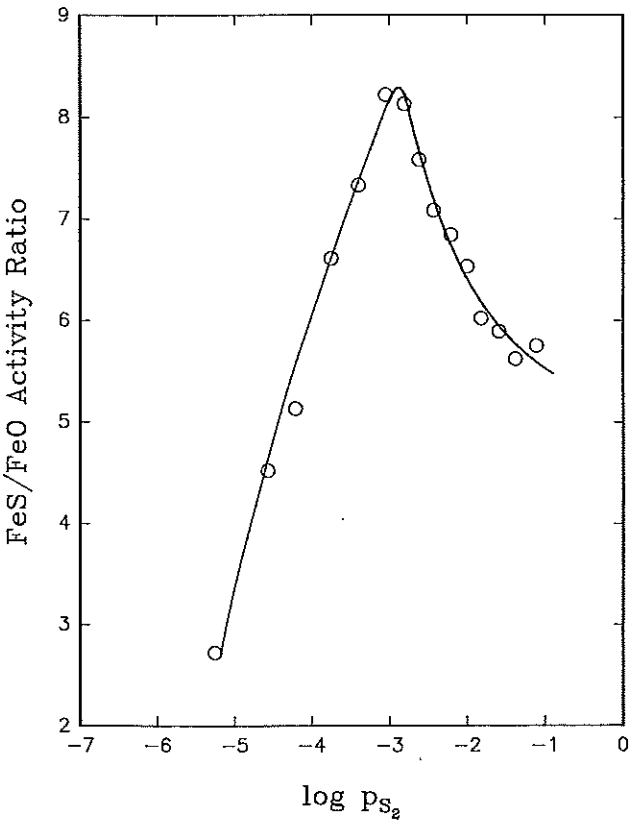

Fig. 12—Variation of the ratio of activities of FeS and FeO along the line YOP in Fig. 11.

APPENDIX

Determination of the Composition of Slag and Oxysulfide Samples

The species in the quenched samples were identified by means of electron microprobe analysis (EMPA) using a JEOL JXA5 microprobe. Seven species were identified. Two representative samples each of slag and matte were then examined in detail using EMPA to obtain their compositions; the results are given in Table A1. The average composition of each of the species was calculated by taking the average of the point analyses for that species and scaling them to 100 pct. The composition of species 1 corresponds to pyrrhotite, and this is present in the samples as the bright areas in Figures 3 and 4. Species 2 was identified as fayalite, and this is present in the samples as the grey or dark-gray matrix areas in Figures 3 and 4. Species 3 is silica in the form of long coarse needles. Because of their size and well-defined shape, it is concluded that these were present in the melt at 1200 °C and did not form during the quench. Species 4, 5, and 7 are not true phases but are eutectic intergrowths and their compositions, therefore, correspond to the average of the individual phases making up the intergrowths. Species 6 corresponds roughly to wustite in composition. It is not present in the photomicrographs in Figures 1 and 2 and was found only on three occasions in a total of 442 point analyses. All the species except wustite were present in the slag samples. Tridymite needles were present in all the oxysulfide samples but in only a few slag samples. The intergrowth species 5 and wustite were not found in any matte samples.

The identification of the species was confirmed by comparing the results with the species identified in the Fe-O-S-SiO_2 system by MacLean.[6] Species 2 and 5 were identified by MacLean as iron silicates, and their composition ranges determined in the present study are in agreement with those given by McLean. McLean identified species 4 and 7 as oxysulfides; species 4 occurred in the matte phase, and species 7 was the eutectic product in the slag phase.

The mineralogical compositions of the melts were determined by covering each photomicrograph with a 1 by 1-mm grid on a transparent plastic sheet. Each photograph was thereby divided into about 2200 small squares of equal area. The number of squares corresponding to each species was next counted, and this was used to obtain the fractional area occupied by each species in the sample. In all cases, the area occupied by the large needle-shaped silica crystals was neglected and the other areas scaled accordingly to give a total of 100 pct.

To convert the area fractions to mass per cent of the various species, it is necessary to assume that the sample is isotropic and to take into account their relative densities. By combining the results for the average composition of each species, the relative areas of each species and the density of each species, the bulk elemental composition of each sample was calculated. The EMPA technique does not permit differentiation between ferric and ferrous iron. Therefore, initially all iron was expressed as ferrous iron and these values were then corrected using a linear regression of the Fe (II)-to-Fe (III)

Table A1. Composition Range and Average Composition of Species in the Quenched Melts

Species	Composition Range (Mol Pct)				Average Composition (Mass Pct)			
	Fe	Si	S	O	Fe	Si	S	O
Pyrrhotite	46.9 to 50	0 to 0.3	48.0 to 51.0	0 to 1.8	63.5	0.03	36.3	0.12
Fayalite	28.9 to 30	13.3 to 14	0 to 0.1	56.5 to 57	55.5	13.3	0.03	31.1
Tridymite	0.1 to 0.3	33.1 to 33.3	0 to 0.01	66.5 to 66.6	0.60	46.4	0.01	53.0
Oxysulfide	46.5 to 49.8	0.1 to 1.9	22.1 to 37.5	13.3 to 28.8	67.8	0.65	22.8	8.79
Intergrowth 1	21.2 to 25.8	16.1 to 19.2	0 to 1.5	57.7 to 59.5	46.6	18.8	0.10	34.5
Wustite	44.6 to 47.9	1.4 to 2.2	0 to 0.2	50.6 to 53	74.5	1.48	0.11	23.9
Intergrowth 2	31.4 to 36.2	9.2 to 12.4	1.2 to 12	42.6 to 53.9	59.2	9.82	5.54	25.4

Table A2. Comparison of Slag and Matte Compositions Determined Using ICP and Image Analysis (IA) (Uncorrected for Silica Contamination)

Experiment Number	Pct SiO_2		Pct ΣFe		Pct S	
	ICP	IA	ICP	IA	ICP	IA
Slag						
13	33.1	28.3	49.6	54.8	3.0	2.3
20	25.7	23.5	53.5	57.6	6.6	4.8
24	26.3	29.1	54.2	54.4	—	1.76
35	28.3	31.4	51.9	52.4	—	2.54
46	27.2	32.0	52.7	52.3	—	1.39
Matte						
50	23.5	16.7	53.5	58.5	10.1	15.2
26	22.0	14.9	54.3	59.7	10.6	16.4
17	21.9	10.3	52.4	63.1	—	16.9
19	20.0	12.9	52.4	61.4	—	16.0

ratio *vs* oxygen partial pressures determined from analyses of ferrous and ferric iron contents on seven slag and oxysulfide samples for which there was a sufficient amount available to perform the analysis.

Of the 59 experiments successfully performed, only 10 cases had sufficient sample recovered to enable chemical analysis to be carried out. This was done using the inductively coupled plasma (ICP) technique. The results are shown in Table A2 which also shows the corresponding results obtained by image analysis. Because the chemical analyses include the silica contamination from the tridymite needles, the image analysis values have been left uncorrected to enable a comparison of the two methods to be made.

In the case of the slag samples, the total iron and silica contents determined by the two methods agree within 10 pct. Only two sulfur analyses were obtained because a separate sample was required for these. These follow the trends of the image analysis results but are considerably larger. The silica contents of the oxysulfide samples determined by ICP are considerably higher than the contents obtained by image analysis. This reflects the choice of area of the sample used for the image analysis measurements; a representative area was chosen in all cases which was relatively free of tridymite needles and crucible contamination. The higher silica content of the ICP results is reflected in the lower total iron and sulfur results by ICP compared with image analysis due to the diluting effect of the tridymite inclusions and crucible contamination. If the difference between the silica analyses by the two methods is assumed to be due to additional silica in the samples analyzed by ICP then an approximate correction can be made by distributing this difference to the total iron, sulfur, and oxygen in proportion to their concentrations. This raises the total iron concentrations by ICP to 58.3 and 59.2 pct and the sulfur concentrations to 11.0 and 11.6 pct for experiments 20 and 24, respectively. The iron concentrations are now in excellent agreement with the image analysis values, but the sulfur concentrations are still low compared with the image analysis values although they follow the same trend.

The number of chemical analyses is too small and the accuracy too uncertain to enable a detailed comparison to be made with the results of the image analysis method. However, they give some confidence that the image analysis values are reliable. Further evidence of the reliability of the image analysis results is their internal consistency. The trends in the values and the effect of various parameters is fully examined in the article. A third test of the reliability of the image analysis results is provided by the consistency of the results when they are extrapolated to conditions that have been investigated previously and for which conventional chemical analyses are available. Few results of this type are available but, as discussed in the article, the present results are consistent with these.

REFERENCES

1. D.C. Hilty and W. Crafts: *Trans. AIME*, 1962, vol. 194, pp. 1307-12.
2. S. Bog and T. Rosenqvist: *The Physical Chemistry of Metallic Solutions and Intermediate Compounds*, Her Majesty's Stationery Office, London, 1959 paper 6B.
3. M. Stofko, J. Schmiedl, and T. Rovenqvist: *Scan. J. Metall.*, 1974, vol. 3, pp. 113-18.
4. Ya.I. Ol'shanskii: *Izv. Akad. Nauk SSSR*, 1951, Geology ser. 6, pp. 128-52.
5. A. Yazawa and M. Kameda: *The Technology Reports of The Tohoku University*, 1953, vol. 18, pp. 40-58; 1955, vol. 19, pp. 1-22, 239-50, 251-61; 1956, vol. 21, pp. 31-50.
6. W.H. MacLean: *Econ. Geol.*, 1969, vol. 64 (8), pp. 865-84.
7. L.S. Darken and R.W. Gurry: *J. Am. Ceram. Soc.*, 1945, vol. 67, pp. 1398-1412.
8. M. Nagamori and M. Kameda: *Trans. Jpn. Inst. Met.*, 1965, vol. 6, pp. 21-30.
9. A. Muan and E.F. Osborn: *Phase Equilibria Among Oxides in Steelmaking*, Addison-Wesley Publishing Co., Reading, MA, 1965.
10. R. Schuhmann: *Chicago Regional Meeting of AIME*, 1951, pp. 1-12.
11. O. Kubaschewski and C.B. Alcock: *Metallurgical Thermochemistry*, 5th ed., Pergamon Press, Oxford, 1979, pp. 378-84.
12. F.Y. Bor and P. Tarassoff: *Can. Metall. Q.*, 1971, vol. 10, pp. 267-71.
13. A. Gevici and T. Rosenqvist: *Trans. Inst. Min. Metall.*, 1973, vol. 82C, pp. 193-201.
14. F.T. Tavera and W.G. Davenport: *Metall. Trans. B*, 1979, vol. 10B, pp. 237-41.
15. P. Spira and N. Themelis: *J. Met.*, 1969, vol. 21, pp. 35-42.
16. A.K. Biswas and W.G. Davenport: *Extractive Metallurgy of Copper*, 2nd ed., Pergamon Press, Oxford, 1980, pp. 92-93.
17. S.N. Sinha and M. Nagamori: *Metall. Trans. B*, 1982, vol. 13B, pp. 461-70.
18. M. Nagamori, T. Hatakeyama, and M. Kameda: *Trans. Jpn. Inst. Met.*, 1970, vol. 11, pp. 190-94.
19. A. Yazawa: *Can. Metall. Q.*, 1974, vol. 13, pp. 443-53.
20. E.J. Michal and R. Schuhmann: *J. Met.*, 1952, vol. 4, pp. 723-28.
21. R. Schuhmann and P.J. Ensio: *J. Met.*, 1951, vol. 3, pp. 401-11.